HHS Public Access

Author manuscript

Cell Metab. Author manuscript; available in PMC 2017 October 11.

Published in final edited form as:

Cell Metab. 2016 October 11; 24(4): 582–592. doi:10.1016/j.cmet.2016.08.012.

Suppressors of Superoxide-H_2O_2 Production at Site I_Q of Mitochondrial Complex I Protect against Stem Cell Hyperplasia and Ischemia-Reperfusion Injury

Martin D. Brand[1,*,7], **Renata L.S. Goncalves**[1,4], **Adam L. Orr**[1,5], **Leonardo Vargas**[2], **Akos A. Gerencser**[1], **Martin Borch Jensen**[1], **Yves T. Wang**[3], **Simon Melov**[1], **Carolina N. Turk**[2], **Jason T. Matzen**[2], **Victoria J. Dardov**[2], **H. Michael Petrassi**[2], **Shelly L. Meeusen**[2], **Irina V. Perevoshchikova**[1,6], **Heinrich Jasper**[1], **Paul S. Brookes**[3], and **Edward K. Ainscow**[2]

[1]Buck Institute for Research on Aging, Novato, CA 94945, USA

[2]Genomics Institute of the Novartis Research Foundation, San Diego, CA 92121, USA

[3]Department of Anesthesiology, University of Rochester Medical Center, Rochester, NY 14642, USA

SUMMARY

Using high-throughput screening we identified small molecules that suppress superoxide and/or H_2O_2 production during reverse electron transport through mitochondrial respiratory complex I (site I_Q) without affecting oxidative phosphorylation (suppressors of site I_Q electron leak, "S1QELs"). S1QELs diminished endogenous oxidative damage in primary astrocytes cultured at ambient or low oxygen tension, showing that site I_Q is a normal contributor to mitochondrial superoxide-H_2O_2 production in cells. They diminished stem cell hyperplasia in *Drosophila* intestine in vivo and caspase activation in a cardiomyocyte cell model driven by endoplasmic reticulum stress, showing that superoxide-H_2O_2 production by site I_Q is involved in cellular stress signaling. They protected against ischemia-reperfusion injury in perfused mouse heart, showing directly that superoxide-H_2O_2 production by site I_Q is a major contributor to this pathology.

[*]Correspondence: mbrand@buckinstitute.org.

[4]Present address: Department of Genetics and Complex Diseases, T.H. Chan Harvard School of Public Health, Boston, MA 02115, USA

[5]Present address: Gladstone Institutes, San Francisco, CA 94158, USA

[6]Present address: BioMarin Pharmaceutical Inc., San Rafael, CA 94901, USA

[7]Lead Contact

SUPPLEMENTAL INFORMATION

Supplemental Information includes Supplemental Experimental Procedures, two figures, and one table and can be found with this article online at http://dx.doi.org/10.1016/j.cmet.2016.08.012.

AUTHOR CONTRIBUTIONS

M.D.B., A.L.O., and E.K.A. devised the project and designed and interpreted the screen. R.L.S.G., A.L.O., L.V., A.A.G., M.B.J., Y.T.W., C.N.T., J.T.M., and V.J.D. carried out the experiments. M.D.B., R.S.L.G., A.A.G., M.B.J., S.M., S.L.M., I.V.P., H.J., P.S.B., and E.K.A. designed, coordinated, and helped interpret different aspects of the cell, organ and fly work. H.M.P. advised on compound selection. M.D.B. drafted the paper. All authors edited and approved the manuscript.

CONFLICTS OF INTEREST

L.V., C.N.T., J.T.M., V.J.D., H.M.P., S.L.M., and E.K.A. were employed by the Genomics Institute of the Novartis Research Foundation during the period of their contribution to this research. M.D.B. has consulted for Seahorse Bioscience. A.A.G. has a financial interest in Image Analyst Software.

S1QELs are tools for assessing the contribution of site I_Q to cell physiology and pathology and have great potential as therapeutic leads.

Graphical abstract

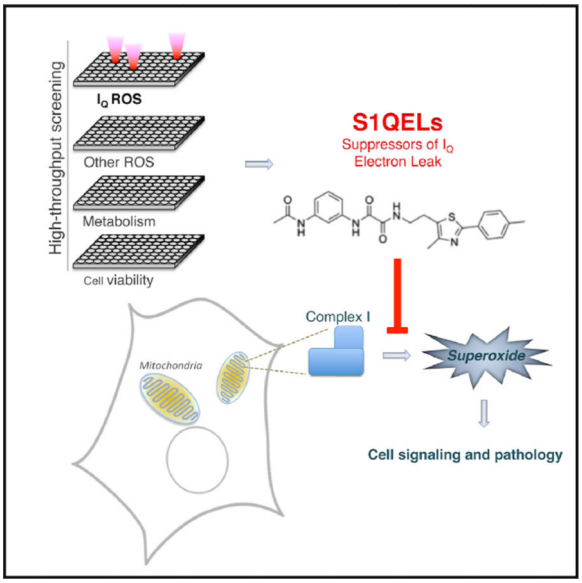

INTRODUCTION

Mitochondria generate ATP by oxidative phosphorylation, but they can also produce reactive oxygen species (ROS) from at least 11 distinct sites associated with substrate oxidation and electron transport (Brand, 2010, 2016; Goncalves et al., 2016; Quinlan et al., 2013a). The relative contributions of these sites differ depending on metabolic context (Brand, 2016; Goncalves et al., 2015; Quinlan et al., 2013b), as do their potential roles in intracellular signaling and oxidative damage (Brand, 2016; Shadel and Horvath, 2015; Sies, 2014). It is likely that mitochondria in resting skeletal muscle produce superoxide and/or H_2O_2 at significant rates from only four of these sites: site I_Q (the site in respiratory complex I active during reverse electron transport, nominally the ubiquinone-binding site), site II_F (the flavin site of complex II), site III_{Qo} (the outer ubiquinone-binding site of complex III), and site I_F (the flavin site of complex I) (Goncalves et al., 2015). Direct evidence for superoxide-H_2O_2 production by site I_Q in cells is lacking (Brand, 2010, 2016; Quinlan et al., 2013a), but indirect evidence links it to longevity (Lambert et al., 2007; Scialò et al., 2016), oxygen sensing by carotid body cells (Fernández-Agüera et al., 2015), and ischemia-reperfusion injury (Chouchani et al., 2014, 2016).

Until very recently, it was difficult to characterize and manipulate superoxide-H_2O_2 production from specific mitochondrial sites because classical respiratory inhibitors or genetic manipulations alter electron flow, which inevitably changes superoxide-H_2O_2 production at other sites and also severely disrupts energy metabolism. To overcome this problem we have identified suppressors of superoxide-H_2O_2 production; these prevent superoxide-H_2O_2 production at specific sites but, crucially, do not affect the underlying

electron flow or oxidative phosphorylation. In a small pilot screen, we identified *N*-cyclohexyl-4-(4-nitrophenoxy) benzenesulfonamide (CN-POBS) as the first suppressor of superoxide-H_2O_2 production at site I_Q (Orr et al., 2013). CN-POBS has a concentration causing 50% inhibition (IC_{50}) of <5 μM, albeit with off-target effects at concentrations greater than ~10 μM. In a much larger screen, we recently identified several suppressors of a different site, III_{Qo}, that have high affinity and selectivity (Orr et al., 2015). These are suppressors of site III_{Qo} electron leak (S3QELs; pronounced “sequels”).

Here, using high-throughput chemical screening and extensive validation, we introduce two different structural classes of compounds that are high-affinity site-specific suppressors of site I_Q electron leak (S1QELs; pronounced “cycles”) but do not interfere with respiration or oxidative phosphorylation. We show that site I_Q is an active contributor to superoxide-H_2O_2 production in cells, isolated organs, and in vivo and that both classes of S1QELs strongly attenuate specific cellular signaling pathways and protect a variety of cells and tissues against damage. In particular, S1QELs protect against stress-induced stem cell hyperplasia in *Drosophila* intestine in vivo and against ischemia-reperfusion injury in perfused mouse heart. By enabling experimental dissociation of superoxide-H_2O_2 production at site I_Q from energy metabolism, S1QELs are unique tools to address the roles of site I_Q in health and disease and hold wide-ranging promise as lead therapeutics.

RESULTS

Identification and Characterization of S1QELs

S1QELs were initially identified using an Amplex UltraRed-based fluorescent H_2O_2 detection assay to screen 635,000 small molecules against H_2O_2 production caused by electron leak at sites I_Q, III_{Qo}, or II_F in isolated muscle mitochondria (Orr et al., 2015). In Orr et al. (2015), we pursued and exploited S3QELs, which suppress at site III_{Qo}. Here, we concentrated instead on site I_Q and eliminated compounds that were unselective for site I_Q or inhibited electron transport or oxidative phosphorylation (Table 1). Two families of compounds, exemplified by S1QEL1.1 and S1QEL2.2 (Figure 1), met our stringent criteria by potently suppressing superoxide-H_2O_2 production specifically at site I_Q without impairing bioenergetic functions in isolated mitochondria or affecting cell growth. The IC_{50} values against superoxide-H_2O_2 production from site I_Q were 0.07 μM for S1QEL1.1 (Figure 1A) and 1.5 μM for S1QEL2.2 (Figure 1H). S1QEL2.1 was the most potent S1QEL2 identified in the screen, with an IC_{50} of 0.29 μM (Figure 1G), but was unavailable for further characterization.

The two families of S1QELs (S1QELs 1.1–1.6 and S1QELs 2.2–2.4) had strict selectivity for site I_Q (Figure 2A). At 10 μM, these S1QELs suppressed superoxide-H_2O_2 production from site I_Q by 40%–85% but did not affect (by >20%–30%) superoxide-H_2O_2 production from site I_F+DH (partly site I_F, but mainly the upstream NAD-linked dehydrogenases, particularly the 2-oxoglutarate dehydrogenase complex, site O_F [Quinlan et al., 2014]), site III_{Qo}, site II_F, or site G_Q (the ubiquinone-binding site of mitochondrial glycerol 3-phosphate dehydrogenase). In isolated mitochondria, S1QELs at 10 μM had no effect on resting respiration (states 2 and 4o) or respiration driving ATP synthesis (state 3) driven by succinate plus rotenone to drive complexes II, III, and IV (Figure 2B). At 20 × IC_{50} against

superoxide-H_2O_2 production by site I_Q, S1QELs also had no effect on respiration driven by glutamate plus malate to drive complexes I, III, and IV (Figure 2C). Thus, the two families of S1QELs were selective suppressors of superoxide-H_2O_2 production by site I_Q, and we found no effects on oxidative phosphorylation in isolated mitochondria, even at 20 × IC_{50} against site I_Q.

Calculation of octanol-water partition coefficients gave predicted $\log_{10}$ (cLogP) values of 2.4 for S1QEL1.1, 5.5 for S1QEL2.1, and 6.3 for S1QEL2.2, suggesting reasonable or high ability of the compounds to enter cells. S1QELs did not inhibit cellular respiration, even when cells had torely solely onmitochondrial metabolism. Basal and uncoupled respiration of HEK293 cells driven by pyruvate, glutamine and galactose were unaffected by exposure for more than 3 hr to high levels of S1QELs (20 × IC_{50} against superoxide-H_2O_2 production by site I_Q in isolated skeletal muscle mitochondria) (Figure 2D). Similarly, the viability ofHEK293 cells was unaffected by exposure for 72 hr to S1QELs at 10 μM or at 20 × IC_{50} against site I_Q (Figure 2E) (except for S1QEL2.4,which was therefore discarded). Thus, the two families ofS1QELs had no effect on oxidative phosphorylation or the viability inHEK293 cells, even at 20 × IC_{50} against site I_Q.

S1QELs Protect Metabolically Resting Primary Astrocytes against Endogenous Oxidative Damage

It is unknown whether site I_Q runs or generates superoxide-H_2O_2 to significant levels in resting cells (Brand, 2016). To explore this issue, we tested the effect of S1QELs on inactivation of succinate dehydrogenase and aconitase activity by the relatively mild oxidative stress experienced by primary astrocytes cultured at 20% or 3% oxygen. Three S1QELs from two different families each increased the succinate dehydrogenase activity of astrocytes above control levels by about 40% during culture at 20% (Figure 3A) or 3% oxygen (Figure 3B). S1QELs tended to increase the total content of succinate dehydrogenase subunit B and ATP synthase subunit β, but this effect was not statistically significant (Figure 3B). Succinate dehydrogenase activity normalized to succinate dehydrogenase subunit B (SDHB) was increased (Figure 3C), consistent with S1QELs diminishing matrix superoxide and therefore decreasing direct inhibition of succinate dehydrogenase activity. Similar protection by S3QELs (Figure 3D) showed that site III_{Qo} also generates matrix superoxide in these cells. The results with S1QELs were corroborated using total cellular aconitase activity. Three S1QELs from two different families each increased the aconitase activity of astrocytes above control levels by about 40% during cell culture (Figure 3E). They also increased citrate synthase activity (Figure 3F), suggesting mitochondrial proliferation. Aconitase activity normalized to citrate synthase still trended higher with S1QEL treatment (Figure 3G), supporting the results with succinate dehydrogenase (Figure 3C), but, in this case, the effect did not reach statistical significance. We draw three important conclusions. First, site I_Q runs in metabolically resting primary astrocytes cultured at 20% or even 3% oxygen and raises superoxide levels enough to cause significant oxidative damage to succinate dehydrogenase. Second, S1QELs are active in these cells—they suppress site I_Q and protect against I_Q-derived endogenous oxidative damage. Third, superoxide-H_2O_2 generated by site I_Q negatively regulates the amount of mitochondria.

S1QELs Protect against Stem Cell Hyperplasia in *Drosophila* In Vivo

To examine the involvement of site I_Q in oxidative stress signaling in vivo and whether such signaling can be suppressed by treatment with S1QELs, we tested the effects of dietary S1QELs on ROS-induced stem cell hyperplasia in live *Drosophila melanogaster*. First, we checked whether two different S1QELs were effective in mitochondria isolated from *Drosophila* and found that they decreased superoxide-H_2O_2 production from site I_Q (Figure 4A) without affecting oxidative phosphorylation (Figures 4B and 4C). We then tested whether S1QELs affect physiological H_2O_2 signaling from site I_Q in vivo using the well-characterized model system of stem cell division in *Drosophila* intestine driven by endoplasmic reticulum (ER) stress. In this model, the ER stressor tunicamycin induces activation of c-Jun N-terminal kinase (JNK) and causes increased ROS production in intestinal stem cells. Intestinal stem cell hyperproliferation is triggered by both elevated ROS and activated JNK, likely through a mitochondrial ROS signal (Biteau et al., 2008; Hochmuth et al., 2011; Wang et al., 2014; Win et al., 2014). Dietary S1QEL1.1 or S1QEL2.2 at 800 nM suppressed the tunicamycin-induced increase in the mitotic marker phospho-histone H3 by up to 45% (Figures 4D and 4E). To check that suppression was not due to effects of S1QELs on feeding and tunicamycin intake, we overexpressed an oncogenic Ras^{V12} mutant that causes ROS-dependent hyperplasia in fly tissues, including intestinal stem cells, without tunicamycin treatment (Biteau and Jasper, 2011; Ohsawa et al., 2012). In this system, S1QELs again decreased hyperplasia (Figure 4F). Control experiments demonstrated that S1QELs did not affect stem cell division in unstressed conditions (Figure 4G) or alter the distribution of cell types in the tissue (see Experimental Procedures). These findings demonstrate that mitochondrial superoxide-H_2O_2 production specifically by site I_Q signals ER stress in intestinal stem cells in vivo and that dietary S1QELs can pharmacologically attenuate this signaling pathway. Similar effects were obtained with S3QEL3 (Figures 4H–4J), showing that site III_{Qo} also contributes to this signaling pathway.

S1QELs Decrease Caspase Activation in a Mammalian Cell Model of ER Stress

Tunicamycin treatment also triggers ER stress and signaling pathways that lead to apoptosis in mammalian cells, and we have shown that S3QELs suppress such signaling through site III_{Qo} in INS-1E insulinoma cells (Orr et al., 2015). To test whether site I_Q is also involved in tunicamycin signaling in mammalian cells, we tested the effects of S1QELs in a cardiomyocyte cell model (H9c2 cells). S1QEL1.1 strongly attenuated caspase activation, and the less-potent S1QEL2.2 also did so at higher concentrations (Figure 5A), showing that site I_Q is involved in the ER stress signaling pathway in these cells. S3QEL2.1 also attenuated caspase activation (Figure 5B), as we previously found in INS-1E cells (Orr et al., 2015), showing that site III_{Qo} also contributes to this signaling pathway in these cells.

S1QEL1.1 Decreases Ischemia-Reperfusion Injury in Perfused Mouse Heart

Chouchani et al. (2014) recently proposed that oxidative damage during cardiac ischemia-reperfusion injury is caused specifically by ROS produced at complex I during reverse electron transport driven by succinate accumulated during ischemia (i.e., site I_Q). To test whether such damage can be suppressed by treatment with S1QELs at the time of

reperfusion, we used the Langendorff-perfused mouse heart model of ischemia-reperfusion injury as previously described (Wojtovich et al., 2013) without and with S1QEL1.1 treatment. S1QEL1.1 had no baseline impact on cardiac function (see Experimental Procedures), suggesting compatibility with complex organ physiology. S1QEL1.1 significantly improved the post-ischemic recovery of cardiac function (rate × pressure product, i.e., heart rate multiplied by left ventricular developed pressure) (Figure 6A) and caused a small but significant decrease in infarct size (Figure 6B). We infer that site I_Q produces damaging superoxide-H_2O_2 during ischemia-reperfusion injury in perfused heart, and treatment with S1QEL1.1 at the time of reperfusion can decrease this production and thus attenuate the oxidative damage.

DISCUSSION

Our high-throughput screen and subsequent counter-screening and validation have identified two independent families of S1QELs (S1QEL1s and S1QEL2s) with the desired properties of low IC_{50} against superoxide-H_2O_2 production by site I_Q in isolated mitochondria, lack of effects on other sites or on oxidative phosphorylation, and the ability to act in cells and organs. Their mechanism of action is unknown, but we speculate that they bind to complex I and alter its conformational flexibility or the redox states of critical electron transport centers. Reverse electron transport is very sensitive to protonmotive force (both membrane potential and ΔpH), and superoxide-H_2O_2 production by site I_Q is exquisitely sensitive to ΔpH (Lambert and Brand, 2004a), both of which are decreased by mild uncoupling. Therefore, we tested extensively for effects on protonmotive force and discarded about 35,000 initial hits that probably worked by mild uncoupling. Specifically, we showed by direct assay that S1QELs do not lower mitochondrial membrane potential (Table 1, steps 3 and 5) or affect state 2 or state 4o respiration, which are even more sensitive to protonmotive force (Figures 2B–2D, 4B, and 4C). Empirically, the assay of site I_F+DH is very sensitive to changes in protonmotive force, and Figure S1 shows how we used that assay to triage all but one of the hits at steps 5–7 of Table 1 and to ensure that the final hits were clean at step 11. Indeed, two compound series (S1QEL3s and S1QEL4s) had some members that affected the I_F+DH assay, so the whole S1QEL3 and S1QEL4 families were discarded late in the screening. The two series that remained, S1QEL1s and S1QEL2s, showed no correlation between potency and any effects of particular members on membrane potential, providing a strong argument that the most active compounds in these series do not work by mild uncoupling.

Using these S1QELs we have made three important discoveries. First, the large increase in succinate dehydrogenase activity (a marker of superoxide in the mitochondrial matrix) caused by S1QELs in primary astrocytes cultured at 3% oxygen provides strong evidence that site I_Q generates superoxide-H_2O_2 at physiologically-relevant rates in resting unstimulated cells. The physiological relevance of site I_Q has been debated ever since high H_2O_2 production from complex I was first demonstrated in isolated mitochondria running reverse electron transport on conventional substrates such as succinate or glycerol 3-phosphate, with most authors considering it to be an interesting in vitro reaction but physiologically insignificant (reviewed by Brand, 2010, 2016; see also Scialò et al., 2016). Primary astrocytes cultured for only 5 days at 3% oxygen are a classic example of resting

unstimulated cells that have not been selected for growth in vitro or exposed to the relatively high oxidative stress of a 20% oxygen atmosphere, yet the effects of S1QELs on this marker of matrix superoxide are significant, showing that site I_Q is generating superoxide in these cells. Whether this site I_Q activity results from reverse electron transport (Lambert and Brand 2004a) or stalled forward electron transport under conditions of adequate substrate availability and low energy demand (Lambert and Brand 2004b) remains to be determined.

Second, the use of S1QELs illuminates roles of superoxide-H_2O_2 production specifically from mitochondrial site I_Q in stress signaling in cells and in vivo. S1QEL inhibition of stem cell hyperplasia in *Drosophila* intestine confirms other evidence that ER stress signaling requires a mitochondrial ROS signal (Hochmuth et al., 2011; Wang et al., 2014). It provides evidence that this signaling uses site I_Q (and the effects of S3QELs show that the signal pathway also uses site III_{Qo}). Similarly, the use of S1QELs and S3QELs shows that these sites are required for mammalian ER stress signaling in insulinoma cells (Orr et al., 2015) and cardiomyocytes (Figure 5). The mechanism by which sites I_Q and III_{Qo} are stimulated is of great interest (see Chambers and LoGrasso, 2011; Win et al., 2014, 2016). Because both S1QELs and S3QELs attenuate this stress signaling, the mitochondrial signal is probably the only cytosolic species they both affect: cytosolic H_2O_2. This is generated directly by endogenous superoxide dismutase 1 from superoxide produced in the cytosol (site III_{Qo}) or indirectly following outward diffusion of H_2O_2 generated from matrix superoxide by superoxide dismutase 2 (sites I_Q and III_{Qo}).

Third, the use of S1QELs provides the first direct evidence for the critical involvement of superoxide-H_2O_2 production specifically from mitochondrial site I_Q in ischemia-reperfusion injury in the heart. Based on metabolite analysis showing accumulation of succinate during ischemia and its rapid oxidation during reperfusion, the protective effects of rotenone, and other indirect lines of evidence, Chouchani et al. (2014, 2016) propose that reverse electron transport through complex I during reperfusion drives ROS production and ischemia-reperfusion injury. The results in Figure 6 showing protection by S1QEL1.1 support their model and suggest a potential therapeutic strategy to protect against such damage caused by excess production of superoxide-H_2O_2 specifically by site I_Q.

We conclude that site I_Q of mitochondrial complex I can generate superoxide and/or H_2O_2 at significant rates in cultured primary cells and cell lines, perfused heart, and intestinal epithelium stem cells in vivo and that the superoxide-H_2O_2 produced by site I_Q is used in signaling and can cause oxidative damage during imposed stresses. S1QELs are cell-permeant and specific suppressors of superoxide-H_2O_2 production by site I_Q and, hence, inhibitors of this signaling and damage. S1QELs provide an exciting way to identify and target signaling and damage caused by mitochondrial production of superoxide or H_2O_2 at site I_Q in biological systems and hold promise for the development of novel therapeutics.

EXPERIMENTAL PROCEDURES

Animals

Female Wistar rats were from Charles River (5–6 weeks old) or Harlan (8 weeks old). Male Sprague Dawley rats were from Taconic Biosciences (8 weeks old). Rat skeletal muscle

mitochondria were prepared as described by Affourtit et al. (2012). Primary astrocytes were isolated from CD1 mice (Charles River). Langendorff-perfusion experiments used male 8–12-week-old C57BL/6J mice (Jackson Laboratory). All animal studies were conducted according to the guidelines of the relevant Institutional Animal Care and Use Committee.

Reagents and Compounds

Reagents were from Sigma-Aldrich unless stated otherwise. The GNF Academic Screening Collection was composed from multiple sources and designed to select for optimal compound properties and eliminate undesirable functional groups (see Table S1). For further assays, S1QELs were obtained from Life Chemicals: S1QEL1.1 (catalog ID F2011-1277), S1QEL1.2 (F2053-0281), S1QEL1.3 (F2053-0279), S1QEL1.4 (F2053-0293), S1QEL1.5 (F2053-0321), S1QEL1.6 (F2011-1334), S1QEL2.2 (F2068-0013), S1QEL2.3 (F2068-0653), and S1QEL2.4 (F2068-0141). The purity of powder stocks was confirmed by high performance liquid chromatograph mass spectrometry (HPLC MS); HPLC purity at 254 nm was greater than 95% and confirmed as molecule as acid (M+H) or molecule as sodium salt (M+Na).S3QELs were obtained as before (Orr et al., 2015). Except where stated otherwise, S1QEL stocks were 10mMin DMSO, with DMSO vehicle controls diluted to the same extent as these stocks. Where a series of S1QELs was used at 20 × IC_{50}, the vehicle control corresponding to the highest IC_{50} was used.

Screening

The overall high-throughput screening strategy and the initial screen (step 1 in Table 1) are described in Orr et al. (2015). A library of ~635,000 compounds was screened at 10 μM in 1,536-well format in assays to identify suppressors of superoxide-H_2O_2 production from sites I_Q, III_{Qo}, and II_F in freshly isolated rat skeletal muscle mitochondria. To identify compounds that selectively suppressed superoxide-H_2O_2 production from site I_Q without affecting oxidative phosphorylation or other superoxide-H_2O_2-producing sites, in the present study we performed a series of triaging assays for selectivity and potency (subsequent steps in Table 1). Superoxide-H_2O_2 production by site I_Q was defined as rotenone-sensitive H_2O_2 production (after dismutation of superoxide by endogenous or exogenous superoxide dismutases) during reverse electron transport from complex II to complex I driven by the oxidation of added succinate in respiratory state 2 (high protonmotive force; no ADP or uncoupler added). H_2O_2 production was measured using the Amplex UltraRed assay (Life Technologies), in which horseradish peroxidase uses H_2O_2 to oxidize non-fluorescent Amplex UltraRed to a highly fluorescent resorufin product. Data were normalized to the plate median signal. Rotenone was included on each plate as a “positive” inhibitor of site I_Q. It inhibited the fluorescent signal by >85%.

Mitochondrial Respiration

Respiration of mitochondria isolated from rat skeletal muscle on 5 mM succinate plus 4 μM rotenone or 5 mM glutamate plus 5 mM malate was assayed in the Seahorse XF24 at 37°C as described in Supplemental Experimental Procedures.

Superoxide Dismutase Activity

S1QELs 1.1, 1.2, 2.1, and 2.2 had undetectable superoxide dismutase activity (< 0.002 U/ml) at 1, 10, and 15 μM using the Cayman Chemical Company Superoxide Dismutase Assay Kit (item No. 706002) and protocol.

Respiration and Superoxide-H_2O_2 Production in *Drosophila* Mitochondria

Drosophila melanogaster (strain Oregon Red) were cultured at 25°C with a 12-hr light-dark cycle on standard yeast and molasses-based food (9% [v/v] molasses; 2.5% [w/v] dry yeast; 0.65% [w/v] agar, and 6.9% [w/v] cornmeal) and used at 10–15 days old. Mitochondria were isolated from ~200 whole flies by homogenizing up to 10 strokes in ice-cold STE (250 mM sucrose, 5 mM Tris-HCl, 2 mM EGTA, pH 7.4) supplemented with 1% (w/v) fatty acid-free bovine serum albumin and then centrifuging as described by Goncalves et al. (2014). Protein was determined by Bradford assay (Biorad). Respiration on 10 mM pyruvate plus 10 mM proline or 10 mM glycerol 3-phosphate plus 2 μM rotenone was assayed in the Seahorse XF24 at 28°C as described in Supplemental Experimental Procedures. To induce superoxide-H_2O_2 production from site I_Q in fly mitochondria, 20 mM glycerol 3-phosphate was added to isolated mitochondria (0.3 mg protein • ml^{-1}) in respiration medium supplemented with 50 μM Amplex UltraRed, 5 U • ml^{-1} horseradish peroxidase and 25 U • ml^{-1} superoxide dismutase. Values were scaled to DMSO as the negative control (100%) and rotenone as the positive control (0%). Fluorescence was monitored using a microplate reader (Pherastar FS, BMG Labtech) at $\lambda_{excitation}$ = 540 nm, $\lambda_{emission}$ = 590 nm.

Cellular Respiration

Respiration of HEK293 cells in the presence of pyruvate, glutamine, and galactose was assayed in the Seahorse XF24 as described in Supplemental Experimental Procedures.

Succinate Dehydrogenase Activity, Aconitase Activity, and Protein Levels in Primary Astrocytes

Succinate dehydrogenase activity is a known target of superoxide in the mitochondrial matrix, which probably directly damages iron-sulfur (FeS) centers and decreases specific activity and indirectly decreases the protein level (Hinerfeld et al., 2004; Melov et al., 1999; Powell and Jackson, 2003). To validate the use of succinate dehydrogenase activity as a probe of matrix superoxide levels, we used primary astrocytes from mice lacking matrix superoxide dismutase, where matrix superoxide levels are elevated, particularly at higher oxygen concentrations, but matrix H_2O_2 levels are presumably lowered. In primary astrocytes from wild-type mice, succinate dehydrogenase activity was unaffected by oxygen level, whereas in astrocytes from mice lacking matrix superoxide dismutase, succinate dehydrogenase activity was decreased to 57% of control at 3% oxygen and to 6% at 20% oxygen (Figure S2), corroborating the conclusion that succinate dehydrogenase activity inversely reflects matrix superoxide levels. The strengths of using succinate dehydrogenase activity as an assay are the specificity for matrix superoxide over hydrogen peroxide (inferred from Figure S2) and the insolubility of the product of the assay reaction, which means that the product marks individual cells and enables the use of microscopy and image processing to measure the activity (and hence matrix superoxide levels) in very small

numbers of cells. No other assay has these advantages of compartmentation, specificity, and sensitivity.

Primary cortical astrocytes were prepared from 3-day-old mouse pups, succinate dehydrogenase activity in adherent cell monolayers was measured by densitometry in an epifluorescence microscope, and expression levels of SDHB and ATP synthase β were assayed as described in Supplemental Experimental Procedures. Aconitase and citrate synthase activity were measured in lysed cells by enzymatic assay as described in Supplemental Experimental Procedures.

In Vivo Stem Cell Proliferation Assays

Drosophila melanogaster were maintained on yeast and molasses-based food at 25°C, unless otherwise noted, with a 12-hr light-dark cycle. To test the effects on tunicamycin-induced stem cell proliferation, w;esgGal4,UAS-GFP; virgins were crossed to Oregon Red males. Six-day old offspring were starved for 4 hr to synchronize feeding, then transferred to5% (w/v) sucrose containing 0.8% (v/v) DMSO and S1QELs at the indicated concentrations. After 24 hr flies were starved for 1 hr, then transferred to the same food containing 50 μM tunicamycin. 24 hr later fly intestines were dissected, stained and imaged. To test effects on Ras^{V12} induced stem cell proliferation, w;esgGal4,UAS-GFP; tubGal80ts virgins were crossed to yw;UAS-Ras^{V12} males at 18°C. 4-day-old offspring were starved for 4 hr to synchronize feeding and then transferred to 5% (w/v) sucrose containing 0.8% (v/v) DMSO and S1QELs at the indicated concentrations. After 24 hr, flies were transferred to 29°C to induce Ras^{V12} expression. Food was supplemented daily for 3 days, then fly intestines were dissected, stained for pH3, and imaged.

Adult female *Drosophila* intestines were dissected in 1× PBS, fixed for 45 min at room temperature (100 mM glutamic acid, 25 mM KCl, 20 mM $MgSO_4$, 4 mM sodium phosphate, 1 mM $MgCl_2$, and 4% [v/v] formaldehyde), washed for 1 hr at 4°C (1× PBS, 0.5% [w/v] bovine serum albumin and 0.1% [v/v] Triton X-100), then incubated with primary antibodies (4°C overnight) and secondary antibodies (4°C for 4 hr or overnight) in washing buffer, washing 3× 10 min after each antibody. For Delta staining, we used methanol-heptane fixation as described by Li et al. (2013).

Using mosaic analysis with a repressible cell marker (Lee and Luo, 2001) to fluorescently label daughter cells arising from a single stem cell over 7 days, we found that S1QELs did not affect stem cell division in unstressed conditions (Figure 4G). MARCM82A:hsFlp,UAS-GFP;;tubGal4,FRT82,tubGal80 virgins were crossed to w;FRT82 males at 18°C. 4-day-old offspring were heat shocked for 45 min at 37°C to induce clone formation, then returned to 18°C. After 7 days, intestines were dissected; stained for Delta, Armadillo, and Prospero; and imaged. We also stained markers of stem cells, enteroblasts, and enterocytes to test for differences in differentiation and/or toxicity and observed no differences in cell type distribution after treatment with S1QELs; ~90% of clones had an identifiable stem cell progenitor with and without S1QELs.

Primary antibodies and dilution are as follows: rabbit anti-phospho-Histone H3 Ser 10 (Upstate, 1:1,000), mouse anti-Armadillo (DSHB, 1:100), mouse anti- Prospero

(Developmental Studies Hybridoma Bank, DSHB, 1:250), and rat anti-Delta (gift from M. Rand, University of Vermont, 1:1,000). Fluorescent secondary antibodies were from Jackson Immunoresearch. DAPI was used to stain DNA. pH3 positive cells were counted manually on a Zeiss dissecting fluorescent microscope; images for clone analysis were taken on a Zeiss LSM 700 confocal microscope and processed using Image J and Adobe Illustrator.

ER Stress Protection Assay

To assess the ability of S1QELs and S3QELs to protect H9c2 rat cardiomyoblasts under ROS-induced cell stress, we induced ER stress using tunicamycin. 8,000 cells were plated per well in a 384-well plate and incubated for 24 hr in 25 μl DMEM with 10% (v/v) FBS. DMSO vehicle (1% v/v) or compounds were added and 0.5 μg • ml^{-1} tunicamycin was added 15 min later. After a further 24 hr, caspase 3/7 activation was measured on a luminometer to quantify relative levels of apoptotic cell death (Caspase Glo 3/7, Promega) (Figure 5). Luminescence with tunicamycin plus S1QELs was normalized to vehicle-treated cells exposed to tunicamycin, following background subtraction of luminescence from cells untreated with tunicamycin.

Cardiac Ischemia-Reperfusion Injury

To assess the effect of S1QEL1.1 in intact mouse hearts, an ex vivo Langendorff-perfusion model of ischemia-reperfusion injury was used (Wojtovich et al., 2013). Following anesthesia with tribromoethanol, the heart was excised then cannulated on a retrograde perfusion system and perfused (4 ml/min constant flow mode) with modified Krebs-Henseleit buffer supplemented with 5 mM glucose, 0.1 mM palmitate/BSA, 1.2 mM lactate, and 0.2 mM pyruvate as respiratory substrates. After equilibration for 20 min, hearts were exposed to 25 min global no-flow ischemia and 60 min reperfusion. At the onset of reperfusion, 0.05% (v/v) DMSO vehicle or S1QEL1.1 (final concentration 1.6 μM, ~20 × IC_{50}) was infused via a port immediately above the perfusion cannula for 5 min. Left ventricular pressure was monitored using a pressure transducer linked to a water-filled polyethylene balloon inserted into the ventricle. A second pressure transducer recorded aortic root pressure. Data was collected digitally (Dataq) at 1 kHz. At the end of reperfusion, hearts were sliced, stained with 1% (w/v) triphenyl tetrazolium chloride (TTC), fixed in formalin, and imaged for quantitation of infarct size.

Before the main experiment, a dosage ramp of S1QEL1.1 was performed in two additional hearts to check for effects on cardiac function. After equilibration, S1QEL1.1 concentrations from 0.08 μM (~1 × IC_{50} against site I_Q in isolated rat skeletal muscle mitochondria) to 1.6 μM (~20 × IC_{50}) were perfused, each for 5 min followed by 10 min wash-out before the next dose. No effect was observed on heart rate, left ventricular systolic or diastolic pressure, or rhythm.

Cardiac function (rate × pressure product) was calculated by multiplying the heart rate by the left ventricular developed pressure averaged over five consecutive beats sampled at various times during perfusion. Data are shown for eight time points: just before ischemia (baseline, 20 min), just before reperfusion (45 min), and every 10 min after the onset of reperfusion until 60 min post-reperfusion. Values for each heart were normalized to the

respective pre-ischemic baseline measurement (set at 100%). Differences between control and S1QEL1.1-treated hearts (n = 6 per group) were compared at each time point by non-paired two-tailed Student's t tests. For each heart, infarct size was measured from 4–6 slices and averaged. Values for control and S1QEL1.1-treated hearts were compared by non-paired two-tailed Student's t test. Both rate × pressure product and infarct size were measured, because it is common to see differences in magnitude of protection by the two measures in cardioprotection studies (Guo et al., 2012).

Statistical Analysis

Unpaired two-tailed Student's t tests or one-way or repeated-measures ANOVA with Dunnett's, Tukey's, or Holm-Sidak's posthoc analysis were used for statistical analysis where indicated.

Supplementary Material

Refer to Web version on PubMed Central for supplementary material.

Acknowledgments

This work was supported by NIH grants R01 AG033542 (to M.D.B.), TL1 AG032116 (to A.L.O.), GM100196 (to H.J.), and R01 HL127891 (to P.S.B.) and The Ellison Medical Foundation grant AG-SS-2288-09 (to M.D.B.). I.V.P. and R.L.S.G. received support from The Glenn Foundation-Buck Institute fellowship program. R.L.S.G. was also supported by the Brazilian Government through the Coordenação de Aperfeiçoamento de Pessoal de Nível Superior (CAPES) e Conselho de Nacional de Desenvolvimento Científico e Tecnológico programa Ciências Sem Fronteiras (CNPq-CSF). M.B.J. was supported by the Alfred Benzon Foundation.

REFERENCES

Affourtit C, Quinlan CL, Brand MD. Measurement of proton leak and electron leak in isolated mitochondria. Methods Mol. Biol. 2012; 810:165–182. [PubMed: 22057567]

Biteau B, Jasper H. EGF signaling regulates the proliferation of intestinal stem cells in Drosophila. Development. 2011; 138:1045–1055. [PubMed: 21307097]

Biteau B, Hochmuth CE, Jasper H. JNK activity in somatic stem cells causes loss of tissue homeostasis in the aging Drosophila gut. Cell Stem Cell. 2008; 3:442–455. [PubMed: 18940735]

Brand MD. The sites and topology of mitochondrial superoxide production. Exp. Gerontol. 2010; 45:466–472. [PubMed: 20064600]

Brand MD. Mitochondrial generation of superoxide and hydrogen peroxide as the source of mitochondrial redox signaling. Free Radic. Biol. Med. 2016 Published online April 13, 2016. http://dx.doi.org/10.1016/j.freeradbiomed.2016.04.001.

Chambers JW, LoGrasso PV. Mitochondrial c-Jun N-terminal kinase (JNK) signaling initiates physiological changes resulting in amplification of reactive oxygen species generation. J. Biol. Chem. 2011; 286:16052–16062. [PubMed: 21454558]

Chouchani ET, Pell VR, Gaude E, Aksentijević D, Sundier SY, Robb EL, Logan A, Nadtochiy SM, Ord EN, Smith AC, et al. Ischaemic accumulation of succinate controls reperfusion injury through mitochondrial ROS. Nature. 2014; 515:431–435. [PubMed: 25383517]

Chouchani ET, Pell VR, James AM, Work LM, Saeb-Parsy K, Frezza C, Krieg T, Murphy MP. A unifying mechanism for mitochondrial superoxide production during ischemia-reperfusion injury. Cell Metab. 2016; 23:254–263. [PubMed: 26777689]

Fernández-Agüera MC, Gao L, González-Rodríguez P, Pintado CO, Arias-Mayenco I, García-Flores P, García-Pergañeda A, Pascual A, Ortega-Sáenz P, López-Barneo J. Oxygen sensing by arterial chemoreceptors depends on mitochondrial complex I signaling. Cell Metab. 2015; 22:825–837. [PubMed: 26437605]

Goncalves RLS, Rothschild DE, Quinlan CL, Scott GK, Benz CC, Brand MD. Sources of superoxide/H_2O_2 during mitochondrial proline oxidation. Redox Biol. 2014; 2:901–909. [PubMed: 25184115]

Goncalves RLS, Quinlan CL, Perevoshchikova IV, Hey-Mogensen M, Brand MD. Sites of superoxide and hydrogen peroxide production by muscle mitochondria assessed *ex vivo* under conditions mimicking rest and exercise. J. Biol. Chem. 2015; 290:209–227. [PubMed: 25389297]

Goncalves RLS, Bunik VI, Brand MD. Production of superoxide/hydrogen peroxide by the mitochondrial 2-oxoadipate dehydrogenase complex. Free Radic. Biol. Med. 2016; 91:247–255. [PubMed: 26708453]

Guo S, Olm-Shipman A, Walters A, Urciuoli WR, Devito S, Nadtochiy SM, Wojtovich AP, Brookes PS. A cell-based phenotypic assay to identify cardioprotective agents. Circ. Res. 2012; 110:948–957. [PubMed: 22394516]

Hinerfeld D, Traini MD, Weinberger RP, Cochran B, Doctrow SR, Harry J, Melov S. Endogenous mitochondrial oxidative stress: neurodegeneration, proteomic analysis, specific respiratory chain defects, and efficacious antioxidant therapy in superoxide dismutase 2 null mice. J. Neurochem. 2004; 88:657–667. [PubMed: 14720215]

Hochmuth CE, Biteau B, Bohmann D, Jasper H. Redox regulation by Keap1 and Nrf2 controls intestinal stem cell proliferation in Drosophila. Cell Stem Cell. 2011; 8:188–199. [PubMed: 21295275]

Lambert AJ, Brand MD. Superoxide production by NADH:ubiquinone oxidoreductase (complex I) depends on the pH gradient across the mitochondrial inner membrane. Biochem. J. 2004a; 382:511–517. [PubMed: 15175007]

Lambert AJ, Brand MD. Inhibitors of the quinone-binding site allow rapid superoxide production from mitochondrial NADH:ubiquinone oxidoreductase (complex I). J. Biol. Chem. 2004b; 279:39414–39420. [PubMed: 15262965]

Lambert AJ, Boysen HM, Buckingham JA, Yang T, Podlutsky A, Austad SN, Kunz TH, Buffenstein R, Brand MD. Low rates of hydrogen peroxide production by isolated heart mitochondria associate with long maximum lifespan in vertebrate homeotherms. Aging Cell. 2007; 6:607–618. [PubMed: 17596208]

Lee T, Luo L. Mosaic analysis with a repressible cell marker (MARCM) for Drosophila neural development. Trends Neurosci. 2001; 24:251–254. [PubMed: 11311363]

Li Z, Zhang Y, Han L, Shi L, Lin X. Trachea-derived dpp controls adult midgut homeostasis in Drosophila. Dev. Cell. 2013; 24:133–143. [PubMed: 23369712]

Melov S, Coskun P, Patel M, Tuinstra R, Cottrell B, Jun AS, Zastawny TH, Dizdaroglu M, Goodman SI, Huang TT, et al. Mitochondrial disease in superoxide dismutase 2 mutant mice. Proc. Natl. Acad. Sci. USA. 1999; 96:846–851. [PubMed: 9927656]

Ohsawa S, Sato Y, Enomoto M, Nakamura M, Betsumiya A, Igaki T. Mitochondrial defect drives non-autonomous tumour progression through Hippo signalling in Drosophila. Nature. 2012; 490:547–551. [PubMed: 23023132]

Orr AL, Ashok D, Sarantos MR, Shi T, Hughes RE, Brand MD. Inhibitors of ROS production by the ubiquinone-binding site of mitochondrial complex I identified by chemical screening. Free Radic. Biol. Med. 2013; 65:1047–1059. [PubMed: 23994103]

Orr AL, Vargas L, Turk CN, Baaten JE, Matzen JT, Dardov VJ, Attle SJ, Li J, Quackenbush DC, Goncalves RLS. Suppressors of superoxide production from mitochondrial complex III. Nat. Chem. Biol. 2015; 11:834–836. [PubMed: 26368590]

Powell CS, Jackson RM. Mitochondrial complex I, aconitase, and succinate dehydrogenase during hypoxia-reoxygenation: modulation of enzyme activities by MnSOD. Am. J. Physiol. Lung Cell. Mol. Physiol. 2003; 285:L189–L198. [PubMed: 12665464]

Quinlan CL, Perevoschikova IV, Goncalves RLS, Hey-Mogensen M, Brand MD. The determination and analysis of site-specific rates of mitochondrial reactive oxygen species production. Methods Enzymol. 2013a; 526:189–217. [PubMed: 23791102]

Quinlan CL, Perevoshchikova IV, Hey-Mogensen M, Orr AL, Brand MD. Sites of reactive oxygen species generation by mitochondria oxidizing different substrates. Redox Biol. 2013b; 1:304–312. [PubMed: 24024165]

Quinlan CL, Goncalves RLS, Hey-Mogensen M, Yadava N, Bunik VI, Brand MD. The 2-oxoacid dehydrogenase complexes in mitochondria can produce superoxide/hydrogen peroxide at much higher rates than complex I. J. Biol. Chem. 2014; 289:8312–8325. [PubMed: 24515115]

Scialò F, Sriram A, Fernández-Ayala D, Gubina N, Lõhmus M, Nelson G, Logan A, Cooper HM, Navas P, Enríquez JA, et al. Mitochondrial ROS produced via reverse electron transport extend animal lifespan. Cell Metab. 2016; 23:725–734. [PubMed: 27076081]

Shadel GS, Horvath TL. Mitochondrial ROS signaling in organismal homeostasis. Cell. 2015; 163:560–569. [PubMed: 26496603]

Sies H. Role of metabolic H_2O_2 generation: redox signaling and oxidative stress. J. Biol. Chem. 2014; 289:8735–8741. [PubMed: 24515117]

Wang L, Zeng X, Ryoo HD, Jasper H. Integration of UPRER and oxidative stress signaling in the control of intestinal stem cell proliferation. PLoS Genet. 2014; 10:e1004568. [PubMed: 25166757]

Win S, Than TA, Fernandez-Checa JC, Kaplowitz N. JNK interaction with Sab mediates ER stress induced inhibition of mitochondrial respiration and cell death. Cell Death Dis. 2014; 5:e989. [PubMed: 24407242]

Win S, Than TA, Min RWM, Aghajan M, Kaplowitz N. c-Jun N-terminal kinase mediates mouse liver injury through a novel Sab (SH3BP5)-dependent pathway leading to inactivation of intramitochondrial Src. Hepatology. 2016; 63:1987–2003. [PubMed: 26845758]

Wojtovich AP, Nadtochiy SM, Urciuoli WR, Smith CO, Grunnet M, Nehrke K, Brookes PS. A non-cardiomyocyte autonomous mechanism of cardioprotection involving the SLO1 BK channel. Peer J. 2013; 1:e48. [PubMed: 23638385]

Highlights

- S1QELs suppress site I_Q ROS production without affecting oxidative phosphorylation
- Site I_Q generates superoxide-H_2O_2 in resting cells and in stress signaling
- Site I_Q drives ischemia-reperfusion injury in perfused heart and S1QELs protect
- S1QELs are tools to assess the contribution of site I_Q and therapeutic leads

In Brief

In this article, Brand et al. identified small molecules (S1QELs) that suppress superoxide-H_2O_2 production during reverse electron transport through mitochondrial respiratory complex I (site I_Q) without affecting oxidative phosphorylation. S1QELs diminished endogenous oxidative damage in primary astrocytes, stress signaling in vivo, and ischemia-reperfusion heart injury.

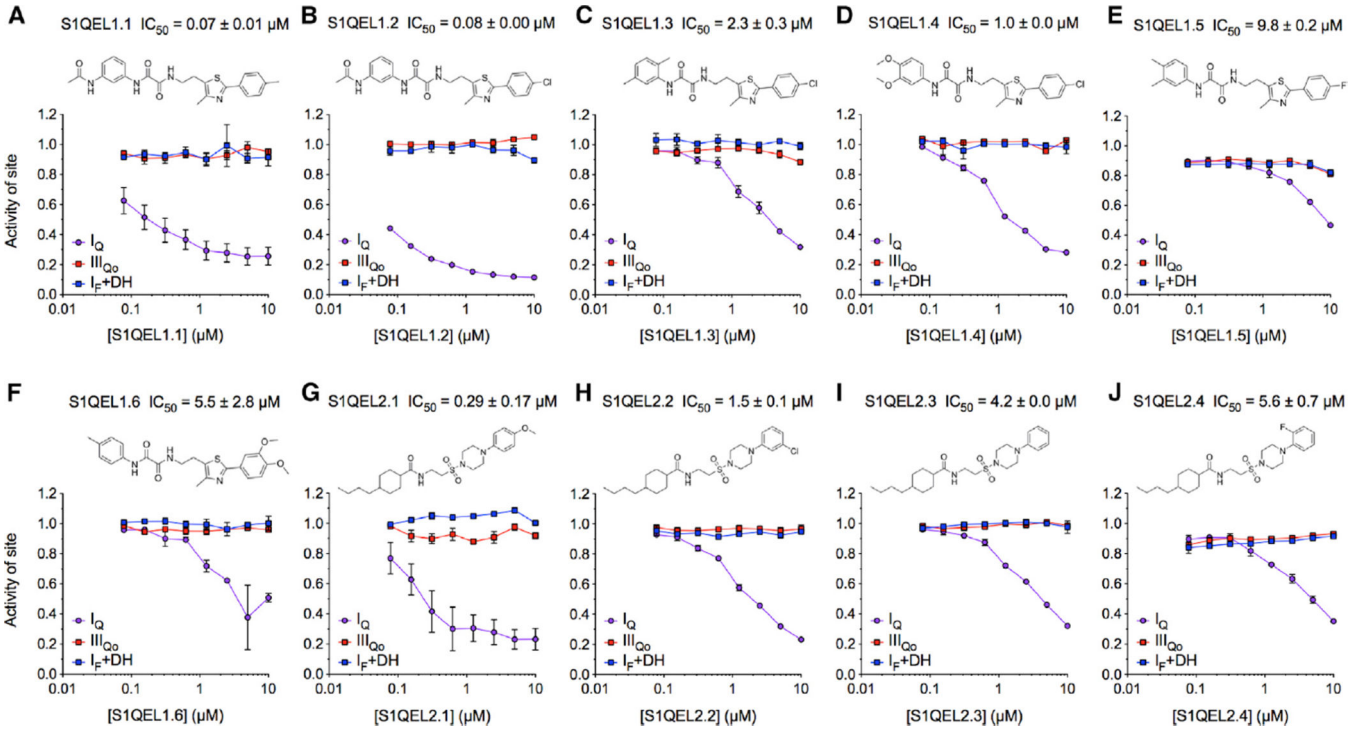

Figure 1. Specific Suppression by S1QELs of Superoxide-H_2O_2 Production from Site I_Q in Isolated Rat Skeletal Muscle Mitochondria

(A–F) Structures of S1QEL1s and dose-response curves against site I_Q (site of respiratory complex I active during reverse electron transport, nominally the ubiquinone binding site), site I_F+DH (flavin site of complex I and predominantly the 2-oxoglutarate dehydrogenase complex, site O_F), and site III_{Qo} (outer ubiquinone-binding site of complex III) normalized to DMSO control = 1.0.

(G–J) Structures of S1QEL2s and dose-response curves.

Data are means ± SE of n = 3 technical replicates (n = 2 for I_F+DH) (step 10 in Table 1). IC_{50} values against superoxide-H_2O_2 production from site I_Q are means ± SE, n = 3 (n = 5 for S1QEL1.1 and S1QEL2.1).

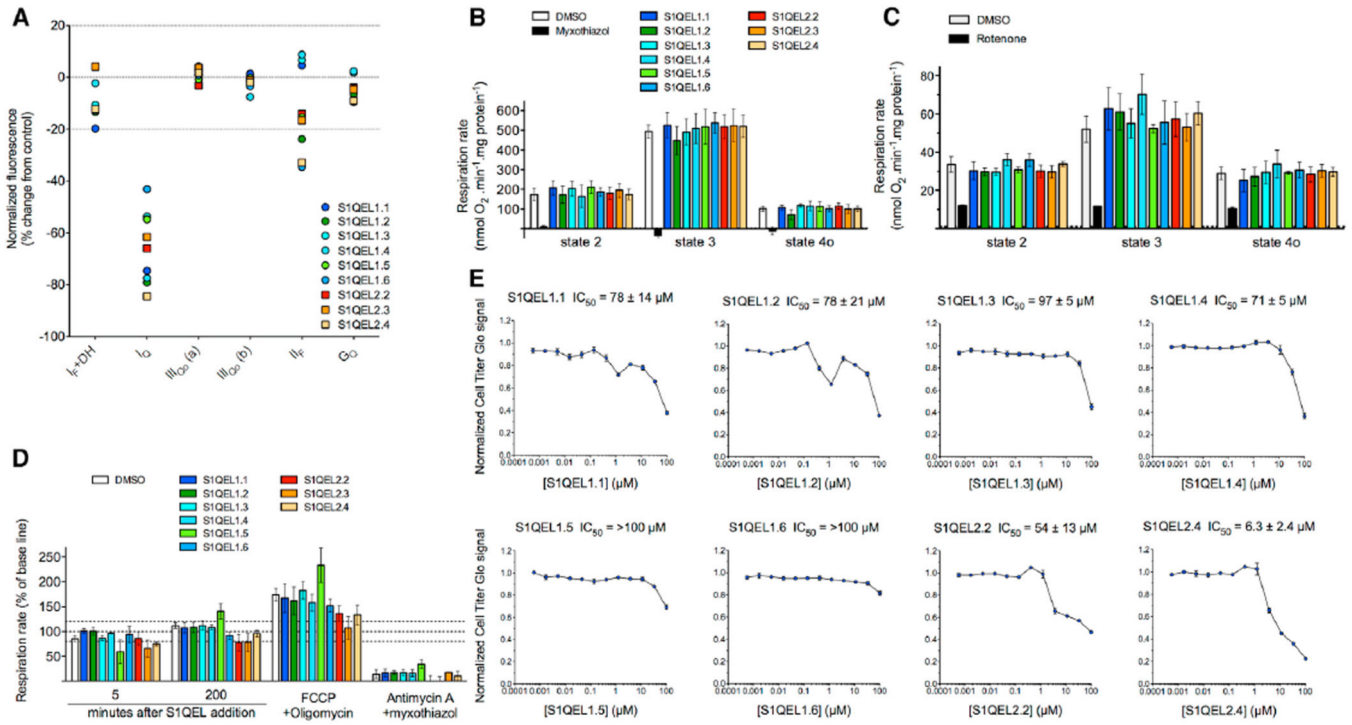

Figure 2. Specificity of S1QELs for Superoxide-H_2O_2 Production from Site I_Q in Isolated Rat Skeletal Muscle Mitochondria without Effects on Oxidative Phosphorylation or Cell Growth

(A) Effects of 10 μM S1QELs on rates of H_2O_2 production from different sites measured by Amplex UltraRed assay (normalized to DMSO control as 0% change and the appropriate positive control [Orr et al., 2013, 2015] as −100%). Dotted lines indicate control and ± 20% changes used to assess specificity. Sites I_Q, I_F+DH, and III_{Qo} are defined in Figure 1; III_{Qo} (a), assay at 5 mM succinate; III_{Qo} (b), assay at 4 mM succinate plus 1 mM malonate; II_F, flavin site of complex II; G_Q, ubiquinone-binding site of mitochondrial glycerol 3-phosphate dehydrogenase. Data are from one experiment.

(B and C) Effect of S1QELs on mitochondrial respiration measured in a Seahorse XF24 driven by (B) 5 mM succinate plus 4 μM rotenone with S1QELs added at 10 μM or (C) 5 mM glutamate plus 5 mM malate with S1QELs added at 20 × IC_{50} against superoxide-H_2O_2 production by site I_Q. Substrate alone (respiratory state 2) was followed by sequential addition of 5 mM ADP (phosphorylating state 3) then 1 μg • ml^{-1} oligomycin (non-phosphorylating state 4o). DMSO was used as vehicle control. 2 μM myxothiazol (in B) and 4 μM rotenone (in C) were controls for conventional inhibition. Data are means ± SE of n = 3 biological replicates (each comprising three technical replicates). Values with S1QELs were not significantly different from values with DMSO (one-way ANOVA).

(D) Effect of S1QELs on respiration of HEK293 cells in the presence of 4 mM pyruvate, 2 mM glutamine, and 20 mM galactose after acute addition of S1QELs at 20 × IC_{50} against superoxide-H_2O_2 production by site I_Q. Where indicated, respiration was uncoupled (and ATPase was inhibited) by addition of 0.6 μM FCCP plus 1 μg • ml^{-1} oligomycin, and non-mitochondrial oxygen consumption was revealed using 4 μM antimycin A plus 4 μM myxothiazol. Data were normalized to baseline in each well before addition of DMSO or S1QEL. Values are means ± SE of three or four biological replicates (each comprising three

technical replicates). Dotted lines indicate the normalized baseline rate and ± 20% changes. Values with S1QELs were not significantly different from values with DMSO (one-way ANOVA).

(E) Effect of S1QELs on growth of HEK293T cells cultured in glucose-free DMEM containing 10% v/v fetal bovine serum, 2 mM pyruvate, 2 mM glutamine, and 20 mM galactose. Cell number was assessed after 72 hr as total ATP measured with Cell Titer Glo. The average effect of compounds was normalized to the intraplate median signal and expressed relative to DMSO control = 1.0. Data are means ± SE (n = 3). IC_{50} values are means ± SD.

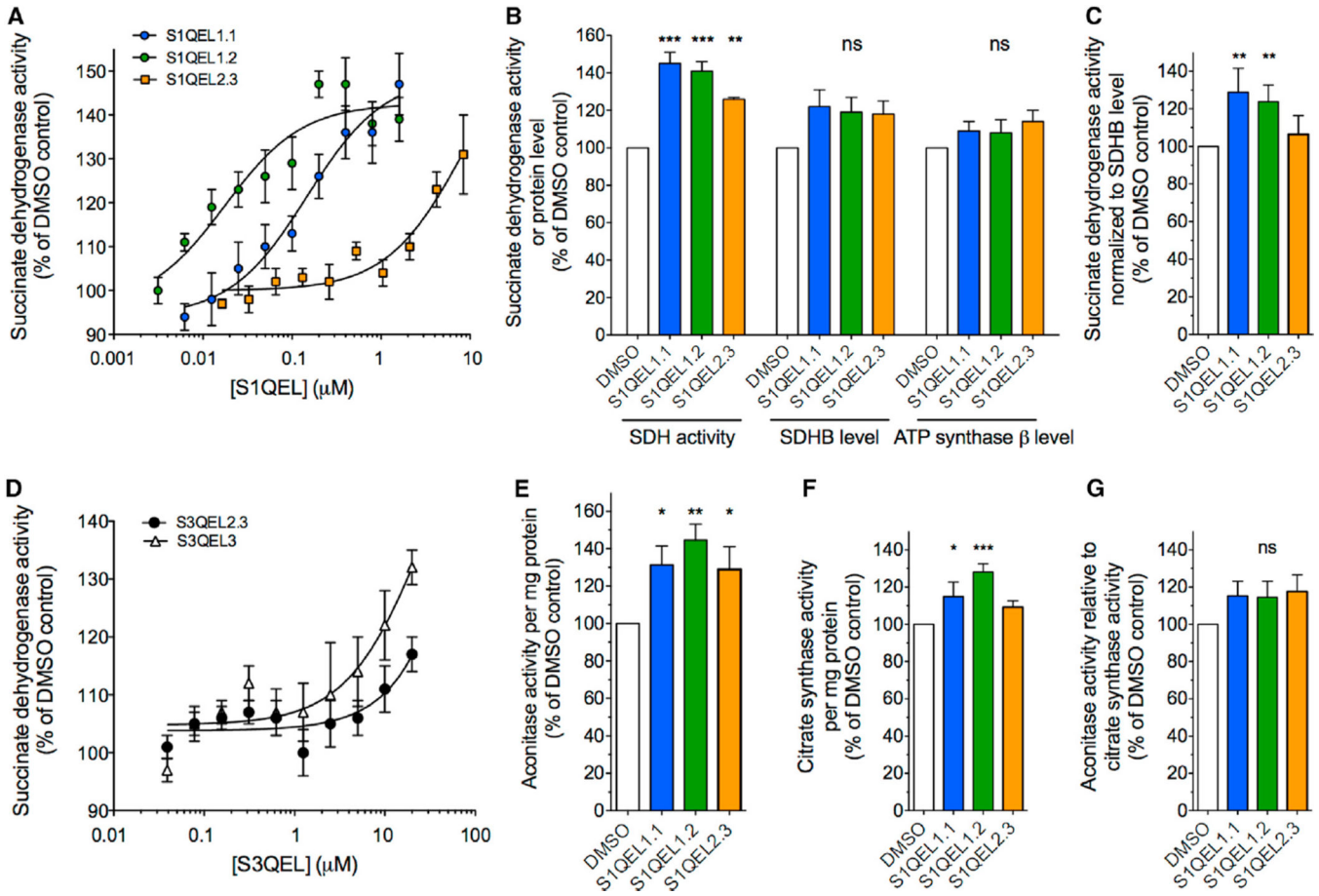

Figure 3. Effects of S1QELs and S3QELs in Primary Cortical Astrocytes

Mouse primary astrocytes were cultured with DMSO vehicle or S1QELs or S3QELs under 3% oxygen for 5 days or 20% oxygen for 3 days.

(A) Titration of succinate dehydrogenase activity in astrocytes cultured with S1QELs under 20% oxygen. Data are means ± SE (n = 5).

(B) Effect of S1QEL1.1 (1.3 μM), S1QEL1.2 (0.2 μM), and S1QEL2.3 (8.4 μM) on succinate dehydrogenase activity and levels of SDH subunit B and ATP synthase β subunit determined by immunofluorescence in astrocytes cultured under 3% oxygen with S1QELs. Data are means ± SE (n = 6).

(C) Effect of S1QELs on succinate dehydrogenase activity normalized to SDH subunit B levels determined by immunofluorescence. Astrocytes were cultured under 3% oxygen in the presence of 1.3 μM S1QEL1.1, 0.2 μM S3QEL1.2, or 8.4 μM S1QEL2.3. Data are means ± SE (n = 4).

(D) Effect of S3QEL2.3 and S3QEL3 on succinate dehydrogenase activity in astrocytes cultured under 20% oxygen in the presence of the compounds. Data are means ± SE (n = 5).

(E–G) Effect of S1QELs on (E) aconitase activity per mg protein, (F) citrate synthase activity per mg protein and (G) aconitase activity/citrate synthase activity in astrocytes cultured under 20% oxygen for 5 days with 0.1% (v/v) DMSO or S1QEL1.1 (0.5 μM), S1QEL1.2 (0.2 μM), or S1QEL2.3 (5 μM). Data are means ± SE (n = 5 for S1QEL1.1; n = 8 for S1QELs 1.2 and 2.3).

In all panels, statistics compare values to the appropriate DMSOcontrol. ns, not significant; *$p < 0.05$; **$p < 0.01$; ***$p < 0.001$ by ANOVA followed by Holm-Sidak's posthoc test.

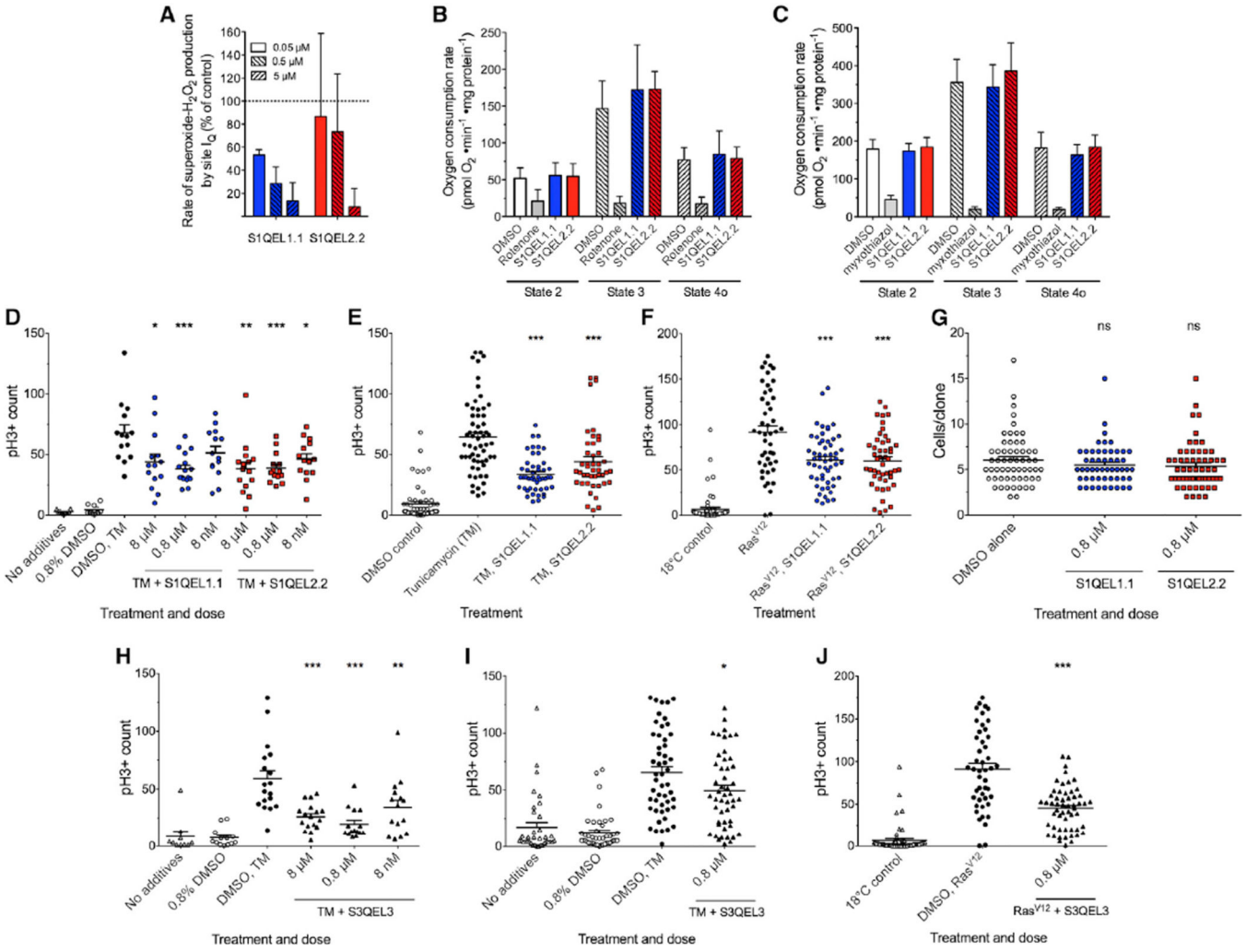

Figure 4. Effects of S1QELs and S3QELs on Mitochondria and Intestinal Stem Cell Hyperproliferation in *Drosophila*

(A–C) Effect of S1QELs 1.1 and 2.2 on mitochondria isolated from *Drosophila*. (A) Superoxide-H_2O_2 production from site I_Q. The 100% value was established in the presence 20 mM glycerol 3-phosphate (dotted line). H_2O_2 production from site I_Q was assumed to be 0% after addition of 5 µM rotenone. (B and C) The effect of S1QEL1.1 and S1QEL2.2 at 20 × IC_{50} (against site I_Q in rat skeletal muscle mitochondria) on respiration rate in *Drosophila* mitochondria driven by (B) 10 mM pyruvate plus 10 mM proline or (C) 10 mM glycerol 3-phosphate is shown. Substrate alone (respiratory state 2) was followed by sequential additions of 1 mM ADP (phosphorylating state 3) and 1 µg • ml^{-1} oligomycin (non-phosphorylating state 4o). DMSO was used as vehicle control. 4 µM rotenone or 2 µM myxothiazol were added as positive controls to show conventional inhibition. Data are means ± SE of three biological replicates (each comprising four technical replicates). Values with S1QELs were not significantly different from values with DMSO (one-way ANOVA). (D–J) Effects of S1QELs (D–G) and S3QELs (H–J) on ROS-dependent induction of stem cell proliferation in vivo in *Drosophila*. S1QELs and S3QELs were administered at the concentrations indicated 24 hr before and during treatments. (D) Dose optimization for

inhibition of stem cell division by S1QELs 1.1 and 2.2, measured by staining of phospho-histone H3 (pH3), following feeding with 0.8% (v/v) DMSO or 50 μM tunicamycin (TM) (final DMSO concentration 0.8% [v/v]). (E and F) Effect of 0.8 μMS1QELs on intestinal stem cell hyperproliferation in vivo in *Drosophila*. Stimulation was measured following (E) 50 μMdietary tunicamycin (TM) or (F) temperature-controlled expression of the Ras^{V12} oncogene. (G) Effect of S1QELs on unstressed stem cell division tracked using the MARCM system to label individual stem cell progeny with GFP. Clone size was assessed at day 7 for 50–60 clones per condition from 6–8 intestines. (H) Dose optimization for inhibition of stem cell division by S3QEL3 (same protocol as D). (I and J) Effect of 0.8 μM S3QEL3 following (I) 50 μM dietary TM or (J) temperature-controlled expression of the Ras^{V12} mutant (same protocols as E and F).

For (D)–(J), horizontal bars show mean ± SE; dots represent individual intestines. ns, not significantly different from DMSO alone; *$p < 0.05$; **$p < 0.001$; ***$p < 0.0001$ versus tunicamycin or Ras^{V12} alone (ANOVA with Tukey's post-test).

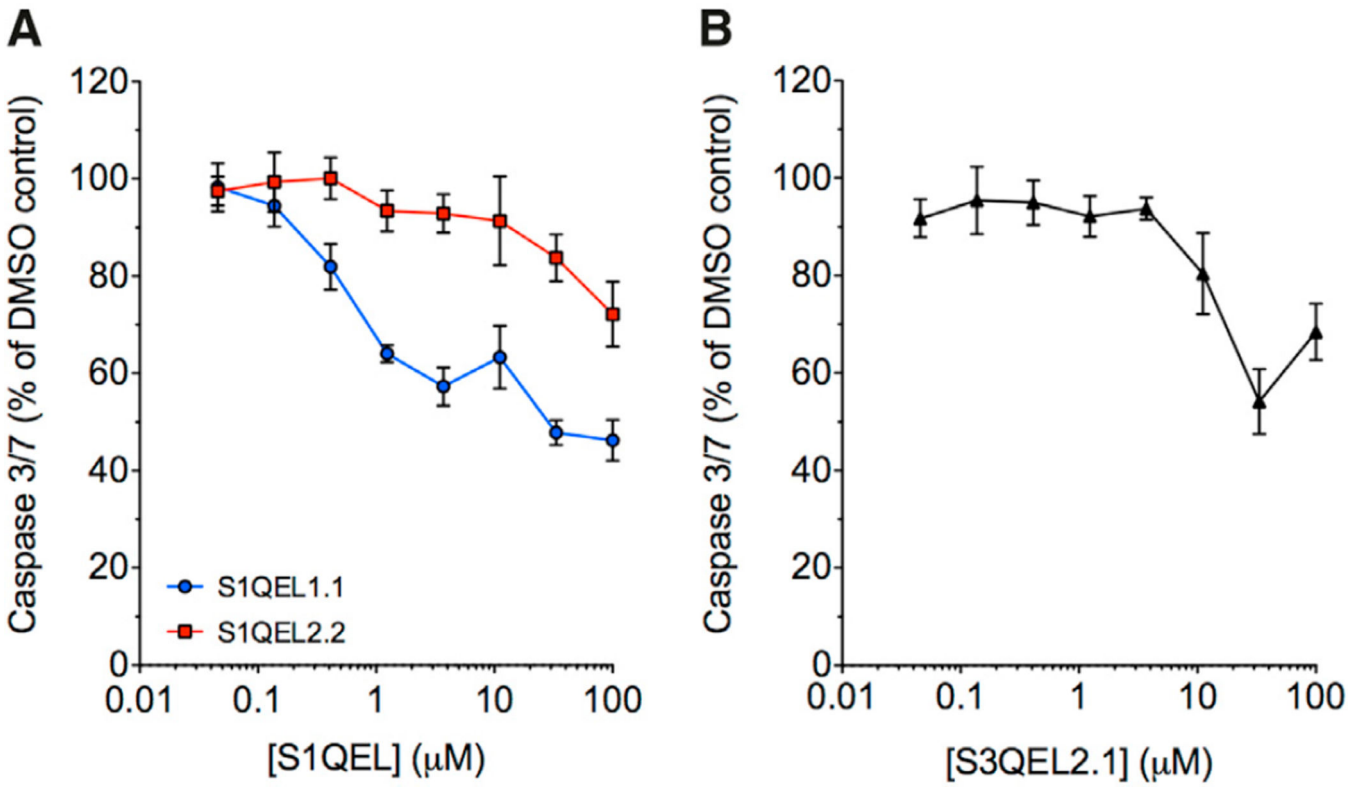

Figure 5. Effects of S1QELs and S3QELs on Activation of Caspase 3/7 by Tunicamycin in H9c2 Cells

(A) Effect of S1QELs.

(B) Effect of S3QEL2.1.

Values are means ± SE, n = 6.

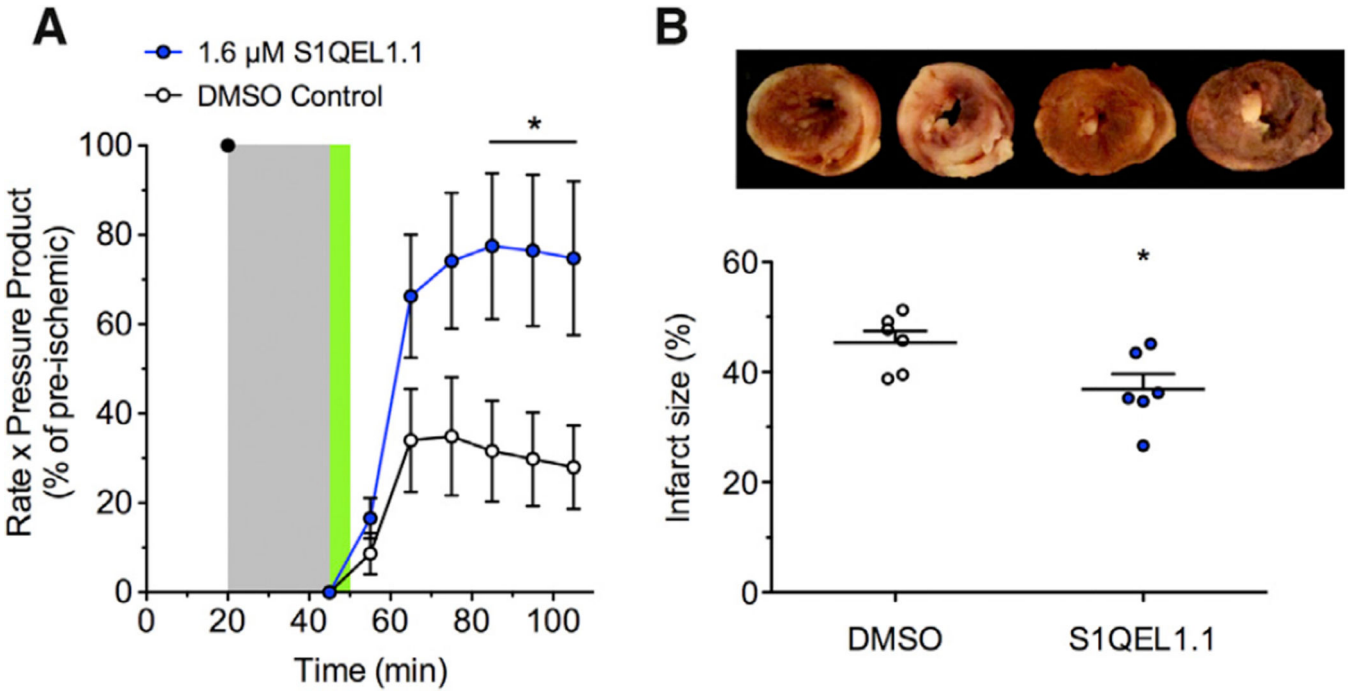

Figure 6. Effect of S1QEL1.1 on Ischemia-Reperfusion Injury in Perfused Mouse Heart

(A) The rate-pressure product in Langendorff-perfused hearts after 20 min equilibration was set to 100%. Flow was stopped for 25 min ischemia (gray). Reperfusion included either 0.05% v/v DMSO vehicle or 1.6 μM S1QEL1.1 for 5 min (green), then continued with no additions.

(B) Infarct size measured at the end of the experiment in the same hearts using tetrazolium chloride staining. Bars are means; dots represent individual hearts. Representative images (white, necrotic infarct; red, live tissue) are shown (left two hearts, DMSO; right two hearts, S1QEL1.1).

Data are means ± SE (n = 6 hearts per group); *p < 0.05 versus control by Student's t test.

Table 1

Screening Strategy to Identify S1QELs

Step	Assay	Description	Concentrations Tested (μM)	Criteria for Selectivity	Remaining Compounds
1	primary screen	endpoint H_2O_2 production from sites III_{Qo}, I_Q, and II_F against 635,000 compounds (Orr et al., 2015)	10	>50% inhibition of I_Q; <45% inhibition of II_F, <50% inhibition of III_{Qo}	34,714
2	cluster selection	clustering of hits by Tanimoto similarity >80%	–	three most active members of each cluster selected	13,555
3	confirmation screen and expanded screens ($\Delta\psi_m$, GalacTox)	endpoint H_2O_2 production from sites III_{Qo}, I_Q, and II_F (triplicate determinations); endpoint $\Delta\psi_m$ assay (TMRM fluorescence); endpoint cell viability after 72 hr exposure	10	>70% inhibition of I_Q; <20% inhibition of III_{Qo}, II_F, TMRM, cell viability; % 1 toxic compound in cluster	3,680
4	dose-response rescreen	determine IC_{50} against I_Q H_2O_2 production (eight-point dose response)	up to 10	progressive inhibition of I_Q (IC_{50} < 0.32 μM)	501
5	expanded rescreen	determine selectivity in six H_2O_2 and two $\Delta\psi_m$ endpoint assays	up to 3.2 (10 × IC_{50} against site I_Q)	>30% suppression of I_Q; <30% inhibition in any other assay	1
6	repopulation of hits and rescreen	add back compounds with IC_{50} against I_Q < 1 μM in step 4, endpoint H_2O_2 production from site I_F+DH	10	<20% inhibition of I_F+DH	511 (including 1 from step 5)
7	expanded rescreen	96-well endpoint H_2O_2 production from sites I_Q, I_F+DH	5	>50% suppression of I_Q; <20% inhibition of I_F+DH	15 (including 1 from step 5)
8	selectivity rescreen	determine selectivity in six H_2O_2 endpoint assays	up to 5 (5 × IC_{50} against site I_Q)	>50% suppression of I_Q >2-fold activity against I_Q than in any other assay (particularly I_F+DH)	8
9	repopulation of hits	add back other members of clusters surviving step 8 identified in step 1 but rejected in step 2	–	–	123
10	dose-response and selectivity rescreen	determine IC_{50} against I_Q, III_{Qo}, and I_F+DH (eight-point duplicate or triplicate determinations)	up to 10	progressive inhibition of I_Q (IC_{50} < 10 μM), <20% inhibition of III_{Qo}, I_F+DH at any concentration	48 (in 6 classes)
11	expanded rescreen	96-well endpoint H_2O_2 production from sites I_Q, I_F+DH, III_{Qo}, G_Q, II_F	10	>50% suppression of I_Q <20% inhibition of any other site (<40% inhibition of II_F)	19 (in 4 classes)
12	respiration	state 2, 3, 4o respiration on succinate + rotenone and on glutamate + malate (Figures 2B and 2C)	10 (succinate plus rotenone) 20 × IC_{50} against site I_Q (glutamate plus malate)	<20% inhibition of state 3; <20% increase in state 4o	9 (in 2 classes): S1QEL1.1–1.6; S1QEL2.2–2.4. (S1QEL2.1 was not tested)

See also Table S1 and Figure S1.